



ELSEVIER

Available online at [www.sciencedirect.com](http://www.sciencedirect.com)

SCIENCE @ DIRECT®

Earth and Planetary Science Letters 236 (2005) 497–504

EPSL

[www.elsevier.com/locate/epsl](http://www.elsevier.com/locate/epsl)

# Soft sediment deformation by Kelvin Helmholtz Instability: A case from Dead Sea earthquakes

Eyal Heifetz<sup>a,\*</sup>, Amotz Agnon<sup>b</sup>, Shmuel Marco<sup>a</sup>

<sup>a</sup>*The Department of Geophysics and Planetary Sciences, Tel-Aviv University, Israel*

<sup>b</sup>*Institute of Earth Sciences, The Hebrew University of Jerusalem, Israel*

Received 24 January 2005; received in revised form 3 April 2005; accepted 14 April 2005

Available online 21 June 2005

Editor: Dr. V. Courtillot

## Abstract

The standard explanation for soft sediment deformation is associated with overturn of inverted density gradients. However, in many cases, observations do not support this interpretation. Here we suggest an alternative in which stably stratified layers undergo a shear instability during relative sliding via the Kelvin–Helmholtz Instability (KHI) mechanism, triggered by earthquake shaking. Dead Sea sediments have long stood out as a classical and photogenic example for recumbent folding of soft sediment. These billow-like folds are strikingly similar to KHI structures and have been convincingly tied to earthquakes. Our analysis suggests a threshold for ground acceleration increasing with the thickness of the folded layers. The maximum thickness of folded layers (order of decimeters) corresponds to ground accelerations of up to 1 g. Such an acceleration occurs during large earthquakes, recurring in the Dead Sea.

© 2005 Elsevier B.V. All rights reserved.

*Keywords:* Kelvin–Helmholtz Instability; Soft sediment deformation; Paleo-earthquake intensity; Dead Sea basin

## 1. Introduction

The ubiquitous stratification in low-energy deposits, where density typically increases with depth, inhibits gravitational instabilities of the Rayleigh–Taylor type. Yet such deposits commonly show structural evidence of mechanical instabilities experienced in the unconsolidated state. Layer-parallel displace-

ments, not uncommon in soft sediments, force shear between layers and possibly drives instabilities of the Kelvin–Helmholtz (KH) type [1]. Layer-parallel shear in post-depositional situations can be driven by a number of mechanisms such as sloping substrates or water flow above the sediments. Yet, soft sediment deformations are observed also on vanishing slopes and at calm water environments. Sediments in the Dead Sea basin provide long environmental records comprising finely laminated layers, radiometrically dated to a precision of tens to hundreds years [2]. Laminated lake deposits, such as in the Quaternary

\* Corresponding author.

E-mail address: [eyalh@cyclone.tau.ac.il](mailto:eyalh@cyclone.tau.ac.il) (E. Heifetz).

Dead Sea, provide spectacular examples for such deformation structures (Fig. 1) [2]. These structures have been tied to strong earthquakes [3–8], providing a source for shear energy. Earthquakes may leave several types of marks on soft laminated beds, including faulting, folding and fragmentation. Counting laminae (thought to represent seasonal deposition) provides a resolution approaching annual that recently enabled matching of particular deformed laminae to historically documented earthquakes [3].

The folding of soft sediments appears at various intensities, seemingly indicating various stages of the deformation. Folding can evolve from a wavy

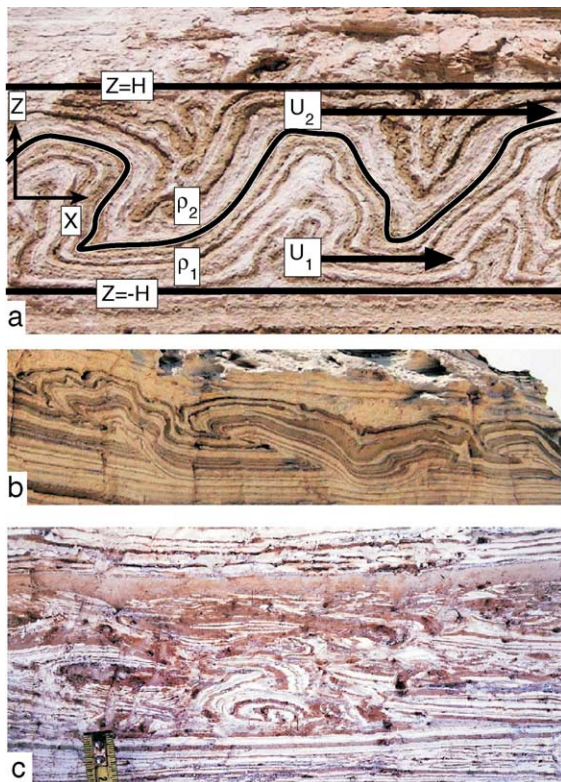


Fig. 1. Examples of different geometry of sediment foldings: (1a) linear wavy geometry, (1b) coherent billow vortices, and (1c) turbulent mixed breccia layer (Photos were taken from the Dead Sea region). In (1a) the speculated original condition supporting KHI is illustrated schematically: Two layers, of thickness  $H$ , initially horizontal and stably stratified ( $\rho_1 > \rho_2$ ), experience an earthquake shaking in the  $x$  direction. In response to the shaking, the denser lower layer moves more slowly than the upper one, forming shear at the interface. The interface, located initially at  $z=0$ , was perturbed becoming unstable with a wavy shape.

shape (Fig. 1a) which can be distorted further to a billow-like or recumbent form (Fig. 1b). The layer may deform further and become fully turbulent, creating a thoroughly mixed breccia layer featuring fragments from the original laminae (Fig. 1c) [3,5,6].

Here we examine the feasibility for a KHI mechanism by which folds are being formed. The shear in the present context is one of fluid flow, not related to the elastic cyclic shear loading prior to liquefaction [9]. KHI was examined in numerous laboratory experiments [10] and numerical simulations [11]. The mechanism involves two horizontal layers that are stably stratified (the light layer overlies the heavy one, Fig. 1a). The layers move horizontally in the same direction but with different speeds, creating shear in the layers' interface. Such shear tends to rotate the beds, giving rise to an instability that uplifts the heavy layer above the lighter one (Fig. 1a). As a result, a wavy structure of billow vortices, distorted by the shear, is formed; the heavier lifted layer tends to collapse into the lighter layer and mix with it (Fig. 1b). If the shear persists, a mixed turbulent boundary layer is developed at the interface where the local shear within the billows forms secondary unstable vortices (note the small scale wiggles in Fig. 1b). These vortices cascade energy into smaller scales and promote the mixing [1] (Fig. 1c).

We attempt to construct a simple physical model to capture the dynamics of the phenomenon (Section 2) and examine its potential instability (Section 3). Finally, we discuss the applicability of the model to Dead Sea deposits (Section 4).

## 2. A simple model of sediment KHI

The folds amount to evidence that deformation took place while the sediment was in a state of unconsolidated mud, reasonably treated as a fluid. During the processes of sedimentation and loss of fluid, the suspension can be viewed as an array of particles falling through the suspending fluid at a steady state velocity. The sedimentation velocity decreases with increasing mass fraction  $\chi$ . Gradients in  $\chi$  tend to form sharp fronts between layers of uniform density, and these fronts travel through the suspension as kinematic waves [12]. Hence, the layers are distin-

guished by mass fraction  $\chi_j$ , of solid material in the sediment. The layers' density is described by

$$\rho_j = \chi_j \rho_s + (1 - \chi_j) \rho_w, \quad (1)$$

where the index  $j$  numerates the layers,  $\rho_s$  is the suspended solid material density and  $\rho_w$  is the suspending fluid density (corresponding to either fresh or salty water). We consider a simple configuration of two neighboring sediment layers  $j=1,2$  (layer-1 underlies layer-2 so that  $\rho_1 > \rho_2$ , Fig. 1a) with thickness  $H$  (A typical value of  $\rho_s = 2500 \text{ kg/m}^3$  where the water density might increase from 1000–1300  $\text{kg/m}^3$  with increasing salinity, for fresh and salty water. A typical value of the fraction in the sediments is  $\chi = 2/3$  and thus Eq. (1) suggests a mean typical density value of the sediments at the range of  $\rho_m = 2000 - 2100 \text{ kg/m}^3$ . The typical fraction difference between two successive sediment layers  $\Delta\chi = \chi_1 - \chi_2$ , is of the order of 0.1 which gives  $\Delta\rho = 150 - 120 \text{ kg/m}^3 \ll \rho_m$ , for both fresh and salty water.). Observations indicate that the typical unstable perturbed wavelength is small compared to the layer interface length but has the same order of the sediment layer width (aspect ratio at the order of unity) [2]. Hence we take for simplicity an infinite horizontal interface (with no vertical boundaries). We consider a case where away from the interface at say  $z = \pm H$  the perturbation vertical velocity vanishes. We assume that the problem is essentially two dimensional (where  $x$  is the direction of the earthquake shaking and  $z$  is the vertical), hydrostatic, incompressible and irrotational away from the interface.

Introducing viscosity to the problem is non-trivial since it is impossible to recover from the present folded sediment layers the original viscosity qualities of the paleo unconsolidated mud before deformation. Moreover, the effective viscosity of a thick suspension under dynamic conditions depends on sizes and shapes of suspended particles. These properties are not well characterized in many natural deposits, and their quantitative effect on viscosity is poorly known. Even if we assume an isotropic viscosity within the layers it is straightforward to show that the viscosity vanishes for an incompressible irrotational flow. Then the viscosity should be incorporated in the internal boundary condition by requiring continuity of the normal stress along both sides of the interface [1]. These normal stress cannot be quantified however,

from present observations. Hence, here we take a simple approach of representing viscosity in terms of the bulk Rayleigh damping [13]:

$$\mathbf{f}_v = -r\mathbf{u}, \quad (2)$$

where  $\mathbf{f}_v$  provides the damping force per unit mass,  $\mathbf{u} = (u, w)$  is the 2-D velocity vector and for a given dominant frequency  $r$  is taken as a constant. Damping should be sufficient to reduce the motion significantly within the time scale of an earthquake duration, however it should not be too strong as to diminish the motion completely. We can estimate the damping by using the response to seismic shear waves, as the attenuation of these would dissipate energy in a manner similar to that of internal gravity waves [14]. The quality factor,  $Q$ , is the ratio between the stored energy and the energy lost during a cycle. Due to the Rayleigh damping the wave amplitude decays as  $\exp(-rt)$  and its energy as  $\exp(-2rt)$ . Hence,  $Q = 2\pi/[1 - \exp(-2r/f)] \approx \pi f/r$ , where  $f$  represents the frequency of the most energetic wave, if we assume  $r/f \ll 1$ . Recent estimates based on in situ measurements for sediments [15], provide typical values of  $Q \sim 30 \pm 20$ , thus suggesting  $r \sim 0.1f$ .

We treat the acceleration perturbation of earthquake waves in the soft sediment as pressure gradients, with a horizontal component  $\Pi = -\frac{\partial p}{\partial x}$ . The pressure gradient force is assumed to be damped by Eq. (2), within the time scale of the duration of strong motion. As a result the layers reach an approximate balance where both layers move in concert but the denser lower layer moves more slowly than the upper one, i.e.

$$rU_j = \frac{\Pi}{\rho_j} \quad (3)$$

( $U_j$  denotes the mean velocity of layer  $j$ ), forming shear at the interface. We are focusing on cases where hindered settling creates minor differences between adjacent layers, hence we assume that  $\Delta\rho \ll \rho_m = (\rho_1 + \rho_2)/2$ . Then Eq. (3) gives

$$\Delta U = \frac{\Pi}{r\rho_m^2} \Delta\rho, \quad (4)$$

where  $\Delta U = U_2 - U_1 > 0$  and  $\Delta\rho = \rho_1 - \rho_2 > 0$ .

Hence, under these simplified assumptions a Kelvin–Helmholtz like configuration of stratified sheared bi-layer is being established within the time scale of

an earthquake. Next we examine the possible modal instability resulted from the KHI mechanism.

### 3. Damped growth of sedimental KHI

We seek normal mode wavelike solutions for the perturbation in the form of  $\exp[ik(x - ct)]$ , where  $k$  is wavenumber and  $c$  is phase speed (which could be complex). Then in the Appendix we derive the damped bounded KHI dispersion relation,

$$c = U_m + i \left( \frac{rH}{2K} \right) \left\{ \pm \left[ 1 + \left( \frac{A}{r} \right)^2 K(K - 2Ri \tanh K) \right]^{1/2} - 1 \right\} \quad (5)$$

where

$$U_m = \frac{\rho_1 U_1 + \rho_2 U_2}{\rho_1 + \rho_2}, \quad K = kH, \\ A = \frac{\Delta U}{H}, \quad N^2 = \frac{g}{\rho_m} \frac{\Delta \rho}{H}, \quad Ri = \left( \frac{N}{A} \right)^2. \quad (6a, b, c, d, e)$$

$U_m$  is density weighted mean velocity,  $K$  is the nondimensional wavenumber scaled by the layers' width  $H$ ,  $A$  can be regarded as the bulk mean shear and  $N$  as the bulk buoyancy (Brunt–Väisälä) frequency. The square of the ratio of the two latter terms is known to be the bulk Richardson number [13].

Modal instability is obtained when the imaginary part of the phase speed,  $c_i$ , of Eq. (5) is positive, possible only for wavenumbers  $K > K_c = 2Ri \tanh K_c$ , which is precisely the explicit criterion for the inviscid case of bounded KHI. Using Eq. (6c,e), the latter condition can also be rewritten in terms of the minimal shear required to make a specific wavelength unstable in a given density stratification, i.e.,  $\Delta U > NH \sqrt{2 \tanh K/K}$ . The difference between the viscid and the inviscid KHI is therefore not in the range of instability but in the exponential growth rate,  $GR = kc_i s^{-1}$ ,

$$GR = \frac{r}{2} \left\{ \left[ 1 + \left( \frac{A}{r} \right)^2 K(K - 2Ri \tanh K) \right]^{1/2} - 1 \right\} \quad (7)$$

which is always smaller than the inviscid KHI growth rate (when  $r=0$ ).

A useful measure for earthquake effectiveness is the ground acceleration imposed by the shaking, commonly normalized by the gravitation acceleration  $g$ . Hence, defining the averaged ground acceleration as  $a = \Pi / \rho_m$ , then using Eqs. (4) and (6c), the condition for instability can be rewritten as  $a/g > (r/N) \sqrt{2 \tanh K/K}$ . The typical perturbed wavelength which is found in the observations (c.f. Fig. 1) has an aspect ratio around unity, i.e.,  $\lambda/H \sim 1$  or  $K \sim 2\pi$  and  $\tanh(K) \approx 1$ . Therefore, the lower limit to the averaged ground acceleration for the development of such perturbations is

$$\frac{a}{g} > \frac{r}{\sqrt{\pi N}} = r \sqrt{\frac{\rho_m H}{\pi g \Delta \rho}}. \quad (8)$$

The threshold for instability increases with damping  $r$  and with the square-root of the layer thickness. The threshold is inversely proportional to the square-root of the density difference suggesting that a high density difference is less stable. By contrast, density difference tends to suppress the inviscid KHI. This somewhat surprising result for the viscid case considered here is solely due to the increasing bulk shear for a given pressure gradient. The growth rate Eq. (7) then takes the form

$$GR = \frac{r}{2} \left\{ \left[ 1 + \left( \frac{A}{r} \right)^2 4\pi(\pi - Ri) \right]^{1/2} - 1 \right\}. \quad (9)$$

Finally, using Eqs. (4) and (6), then Eq. (9) can be rewritten explicitly in terms of  $(H, a/g)$

$$GR = \frac{r}{2} \left\{ \left[ 1 + \left( \frac{2\pi g \Delta \rho}{r^2 \rho_m H} \right)^2 \left( \frac{a}{g} \right)^2 - \frac{r^2 \rho_m}{\pi g \Delta \rho} H \right]^{1/2} - 1 \right\}. \quad (10)$$

Fig. 2 shows the calculated growth rate (normalized by the frequency of the dominant seismic wave) as a function of  $(H, a/g)$ . For this example we take typical values of the Dead Sea sediment composition. The solid material, with density  $\rho_s = 2500 \text{ kg/m}^3$ , is suspended into salty water with density  $\rho_w = 1200 \text{ kg/m}^3$ . The averaged suspended mass frac-

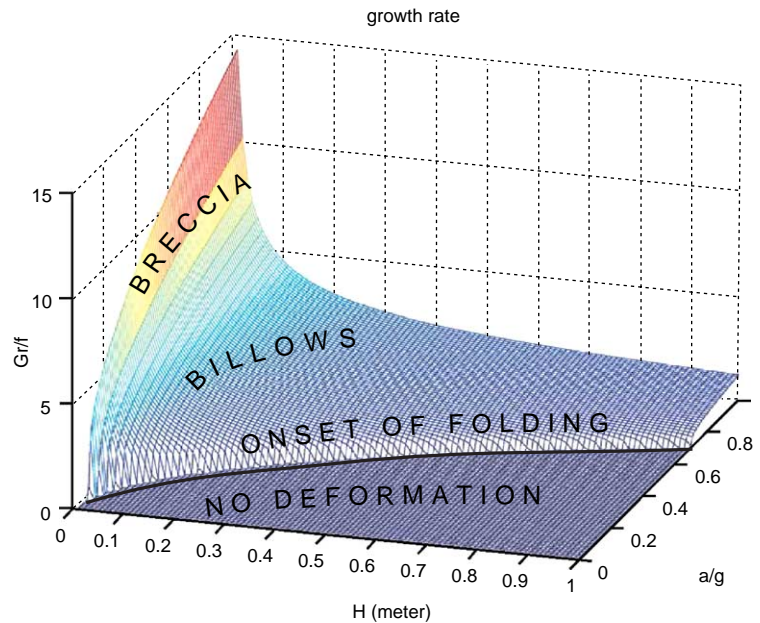


Fig. 2. An example for the KHI growth rate, normalized by frequency  $f$ , as a function of the layer thickness  $H$ , and the normalized ground acceleration  $a/g$ , as given by (10). Here we take typical values of the Dead Sea sediment composition (c.f. text) of  $\rho_m = 2000 \text{ kg/m}^3$ , and  $\Delta\rho = 130 \text{ kg/m}^3$ . The damping coefficient is taken as  $r = 0.1 \text{ Hz}$ . The parabolic solid line marks the threshold for instability (c.f. 8). For onset of linear KHI wave folding (as in Fig. 1a), the growth rates must be in the order of the driving seismic wave frequency (order of 1 Hz). Coherent billows (Fig. 1b) require high growth rates, where fully turbulent mixing, leading to breccia layers (Fig. 1c), requires yet higher growth rates.

tion,  $\chi_m$ , and its difference between the layers,  $\Delta\chi$ , are  $2/3$  and  $0.1$ , respectively, yielding  $\rho_m \approx 2000 \text{ kg/m}^3$ , and  $\Delta\rho = 130 \text{ kg/m}^3$ . The damping coefficient was taken as  $r = 0.1f$ , where the frequency of the most energetic seismic waves  $f$  was taken as  $1 \text{ Hz}$ . The layers are stable for ground accelerations  $a$ , smaller than  $0.07\sqrt{Hg}$  (where  $H$  is in meters), c.f. the parabolic threshold solid line and Eq. (8). For onset of linear KHI wave folding (as in Fig. 1a), the growth rates must be in the order of  $f$ . Coherent billows (Fig. 1b) require high growth rates, where fully turbulent mixing, leading to breccia layers (Fig. 1c), requires yet higher growth rates. For example, for an acceleration  $a = 0.7g$ , layers of  $1 \text{ m}$  thickness or thicker are stable. Thinner layers become unstable, yet for thickness larger than about half a meter, the growth rate might not suffice for the development of instability during the seismic wave half-period. Billow structures can develop in layers with a thickness of fractions of a meter, while fully turbulent mixing is expected for layers with thickness of the order of centimeters.

#### 4. Discussion

Laminated fine-grained sediments, deposited on horizontal bottom under low-energy conditions, are expected to be stably stratified, so density increases with compaction and hence with depth. Since gravitational Rayleigh–Taylor instabilities are not likely under these conditions, alternative mechanisms should be at work. From an observational aspect, the striking similarity of structures in fine-grained laminated deposits to KHI billows, suggests that shear plays a central role in soft sediment deformation (For example, Fig. 3 is a photograph of KHI billow clouds taken in New Zealand during the summer. An atmospheric inversion layer yields both strong stratification and wind shear which together enable KHI to develop. Please note the similarity between Figs. 1b and 3.).

The simple analysis presented here examines the feasibility of KHI in stably stratified sediments. We contend that shear energy is available in various depositional settings such as sloping substrate, high water energy environment, or earthquake prone



Fig. 3. Kelvin Helmholtz billow clouds in the New Zealand summer sky. The clouds are formed along an atmospheric inversion layer (of strong stratification, where temperature increases with height). The inversion layer tends to isolate the surface boundary layer wind from the free atmosphere above it and as a result a shear is formed along the inversion layer. The combination of shear, stratification and humidity provides the conditions for KHI billow clouds to develop. The photo was taken by Mr. Attay Harkabi on January 2001.

regions. We focus here on earthquake related settings, yet the analysis is valid for other scenarios, as long as the pressure gradients are known.

The application of the model to earthquake settings is based on a translation of the instrumentally measurable ground accelerations to pressure gradients. As a preliminary model it does not provide precise correspondence between field observations and the actual driving ground accelerations. Moreover, we cannot rule out alternative sources for pressure gradients, such as surface and internal waves in the depositing water body.

In deriving the model we have neglected differential displacement between grains and suspending fluid. Such displacement is evident in the very existence of billows in sedimentary rocks. While KHI are very common in our surroundings, the resulting structures are ephemeral due to the stabilizing force of gravity. By contrast, billows are so well preserved in sediments due to water loss and consolidation shortly after the onset of the instability. We assume here that on the time scale of development of KHI, the differential displacement between grains and suspending fluid is negligible, yet in the time scale of attenuation of the seismic energy, the differential displacement is sufficient to preserve some of the structure.

Tentative evidence for such differential displacement can be seen in Fig. 1c. [5] have interpreted such structures as a case for differential displacement between grain and water during shaking. Water loss in the lower cohesive zone to the overlying homogeneous zone may have provided upward flow to completely suspend this zone.

The analysis assumes that all displacement fields are confined to a vertical plane. This assumption is valid away from the earthquake source, where  $P$ ,  $S$ , and surface waves have dispersed sufficiently. Some of the most photogenic cases of billows in the Dead Sea laminated deposits indeed show such two-dimensional displacement fields. In the vicinity of the earthquake source, the displacement field is three dimensional, and a more complete analysis is required. At the same time, well documented three dimensional observations will be useful for the study of the vicinity of the earthquake source.

The introduction of bulk damping to represent viscosity, a key simplification of the present analysis, assumes that the viscous damping of the suspension is proportional to the velocity. This representation bypasses the formidable challenge of assessing the effective viscosity under the dynamic conditions of shaking of a thick suspension, in which the suspended particles exhibit a wide range of shapes and scales [16]. The advantage in the present formulation is that the actual coefficient of damping can be estimated from direct experimental observations in a shaking tank. In the absence of such experimental data, we parametrize the bulk Rayleigh damping coefficient in terms of the driving frequency dominant in the acceleration spectrum of the earthquake. The time scale for damping should be sufficiently short as to balance the driving pressure gradient during the time around peak acceleration, say a tenth of the acceleration cycle. This is the rationale behind choosing a bulk Rayleigh friction coefficient 10 times the frequency. The estimation of damping is

also in agreement with the attenuation of seismic shear waves, as the attenuation of these would dissipate energy in a manner similar to that of internal gravity waves [14].

The force balance between the driving pressure gradient and Rayleigh damping yields an expression for the mean shear between the two layers Eq. (4), turning out proportional to the density difference. This leads to the somewhat nonintuitive result that damped KHI increases with the density difference Eq. (8). This result is only valid in the range of small density difference (with respect to the mean density), a range in which Eq. (4) results from Eq. (3). Hence high density difference cannot lead to instability at low acceleration. The prediction of Eq. (8), namely that the instability is promoted by increasing the density difference (at the low range of  $\Delta\rho/\rho_m$ ) can be subjected to experimental verification.

The ability of the analysis to rationalize field observations suggests that KHI is a plausible mechanism for deformation of stably stratified soft sediments. Earthquake-triggered KHI seems plausible for deposits laid horizontally in calm water, as the case is for the earthquake prone Dead Sea basin. The present study sets a foundation for quantitative analysis of deformation structures in laminated sediments and for the extraction of dynamic conditions during earthquakes. This can be a contribution to earthquake science and hazard assessment.

Our analysis indicates that density inversion is not required from the physics of earthquake-induced soft sediment deformation. By extension, we expect that the Kelvin–Helmholtz will provide explanations to common geophysical situations, where gravitational instabilities are inhibited by density stratification. These may include the emplacement of ophiolites, mixing of the upper mantle with the denser lower mantle, and entrainment by hot plumes of dense slugs at the core mantle boundary.

## Acknowledgements

We thank Beny Begin for a constructive review. A. Agnon thanks the German–Israel Binational Science Foundation (GIF) for support. S. Marco was supported by an Israel–US Binational Science Foundation grant #286/97.

## Appendix A. Bounded modal KHI in the presence of Rayleigh damping:

Writing the 2-D Navier–Stokes [1] in the equation,  $\mathbf{f}$  should become  $\mathbf{f}_v$  as defined in Eq. (2).

$$\frac{\partial \mathbf{u}}{\partial t} + \omega \times \mathbf{u} + \nabla \frac{|\mathbf{u}|^2}{2} = -\frac{1}{\rho} \nabla p - \nabla \Phi + \mathbf{f}, \quad (\text{A.1})$$

the vorticity  $\omega = \nabla \times \mathbf{u}$ ,  $p$ ,  $\rho$ ,  $\Phi = gz$ , are the pressure, density and the gravitation potential.  $t$  denotes time and  $\nabla = (\partial_x, 0, \partial_z)$ . The viscosity,  $\mathbf{f}_v$ , is given by Eq. (2). We assume a mean hydrostatic balance in the vertical direction and a mean horizontal balance in the form of Eq. (3).

We seek normal mode wavelike solutions for the perturbation in the form of  $\exp[ik(x-ct)]$ . Everywhere except at the interface, the layers are assumed irrotational,  $\omega=0$ . While the normal modes result from the basic state vorticity  $\delta$ -function on the interface, the companion set of solutions of the continuous spectrum results from rotation within the layers. The continuous spectrum is neutral and therefore traditionally neglected in the context of linear stability. However, due to non-orthogonality between the continuous spectrum and the normal modes, an interaction between the two sets of solutions might lead to a super non-modal growth in finite time [17]. This sort of growth mechanism is however beyond the scope of this work. The modal velocity can be written then in terms of the velocity potential  $\psi$ ;  $\mathbf{u} = -\Delta\psi$ . Then Eq. (A.1) can be rewritten in the barotropic gradient form:

$$\nabla \left[ -\left( \frac{\partial \psi}{\partial t} + r\psi \right) + \left( \frac{|\mathbf{u}|^2}{2} + \frac{p}{\rho} + \Phi \right) \right] = 0, \quad (\text{A.2})$$

and Eq. (2) has been used to represent the viscosity. Eq. (A.2) implies that

$$-\left( \frac{\partial \psi}{\partial t} + r\psi \right) + \left( \frac{|\mathbf{u}|^2}{2} + \frac{p}{\rho} + \Phi \right) = F(t), \quad (\text{A.3})$$

where  $F(t)$  is some function of time only. The LHS of Eq. (A.3) can be regarded as the Rayleigh viscid unsteady flow generalization of the Bernoulli conservation (indicated by the second brackets of the LHS). Assuming also incompressibility of the layers

( $\nabla \mathbf{u}_i = 0$ ) and decomposing the perturbation from the basic state so that  $\mathbf{u}_i = (U_i + u'_i, 0, w'_i)$ , prime indicates the perturbation, then  $\psi_i = -U_i x + \hat{\psi}'_i$ . Writing  $\hat{\psi}'_i = \tilde{\psi}'_i(z) \exp[ik(x - ct)]$ , the incompressibility constraint yields the Laplace equation for the perturbation streamfunction ( $\nabla^2 \tilde{\psi}'_i = 0$ ).

The boundary conditions of vanishing the vertical velocity on the horizontal outer boundaries of the layers, located at  $z = \pm H$ , give the solution:

$$\tilde{\psi}'_i(z) = \frac{\hat{\psi}'_i}{\cosh(kH)} \cosh[k(H - |z|)], \quad (\text{A.4})$$

where  $\hat{\psi}'_i$  is the perturbation's velocity potential amplitude on the two sides of the interface at  $z=0$ . Before and after the time when the perturbation is initiated the pressure on both sides of the interface should be even. This allows us to set the time function  $F(t)$  by using the latter condition in Eq. (A.3) at  $z=0$ , prior to the perturbation:

$$\frac{1}{2}(\rho_1 U_1^2 - \rho_2 U_2^2) = (\rho_1 - \rho_2)F(t), \quad (\text{A.5})$$

which suggests  $F(t)$  to be taken as constant. Perturbing the interface with a vertical displacement  $\zeta' = \hat{\zeta} \exp[ik(x - ct)]$ , linearizing the kinetic energy  $|\mathbf{u}_i|^2/2 \approx U_i^2/2 - \frac{\partial \hat{\psi}'_i}{\partial x} U_i$ , then pressure continuity across the perturbed interface, together with Eqs. (A.3-5), yield

$$\begin{aligned} \rho_1 [ik(U_1 - c)\hat{\psi}'_1 + r\hat{\psi}'_1 - g\hat{\zeta}] \\ = \rho_2 [ik(U_2 - c)\hat{\psi}'_2 + r\hat{\psi}'_2 - g\hat{\zeta}]. \end{aligned} \quad (\text{A.6})$$

In order to obtain the dispersion relation we also imply that the vertical velocity at  $z=0$  is equal to the Lagrangian time derivative of the interface vertical displacement,

$$w(z=0) = \left( \frac{\partial}{\partial t} + \mathbf{u} \cdot \nabla \right) \hat{\zeta}. \quad (\text{A.7})$$

Next we linearize the RHS of Eq. (A.7) with respect to the basic state. Recall that  $w = -\partial \psi' / \partial z$ , we can then write for the two sides of the interface

$$\begin{aligned} \tanh(kH)\hat{\psi}'_1 &= -i(U_1 - c)\hat{\zeta}, \\ \tanh(kH)\hat{\psi}'_2 &= -i(U_2 - c)\hat{\zeta}. \end{aligned}$$

Using that  $\Delta \rho \ll \rho_m$ , Eqs. (A.6) and (A.8) provide the dispersion relation of Eq. (5).

## References

- [1] P.G. Drazin, W.H. Reid, Hydrodynamic Stability, Cambridge University Press, New York, 2004, 626 pp.
- [2] R. Ken-Tor, A. Agnon, Y. Enzel, S. Marco, J.F.W. Negendank, M. Stein, High-resolution geological record of historic earthquakes in the Dead Sea basin, *J. Geophys. Res.* 106 (2001) 2221–2234.
- [3] C. Migowski, A. Agnon, R. Bookman, J.F.W. Negendank, M. Stein, Recurrence pattern of Holocene earthquakes along the Dead Sea transform revealed by varve-counting and radiocarbon dating of lacustrine sediments, *Earth Planet. Sci. Lett.* 222 (1) (2004) 301–314.
- [4] Z.H. El-Isa, H. Mustafa, Earthquake deformations in the Lisan deposits and seismotectonic implications, *Geophys. J. R. Astron. Soc.* 86 (1986) 413–424.
- [5] S. Marco, A. Agnon, Prehistoric earthquake deformations near Masada, Dead Sea Graben, *Geology* 23 (8) (1995) 695–698.
- [6] S. Marco, M. Stein, A. Agnon, H. Ron, Long term earthquake clustering: a 50,000 year paleoseismic record in the Dead Sea Graben, *J. Geophys. Res.* 101 (B3) (1996) 6179–6192.
- [7] B.Z. Begin, D.M. Steinberg, G.A. Ichinose, S. Marco, A 40,000 years unchanging of the seismic regime in the Dead Sea rift, *Geology* 33 (2005) 257–260.
- [8] Y. Enzel, G. Kadan, Y. Eyal, Holocene earthquakes inferred from a fan-delta sequence in the Dead Sea graben, *Quat. Res.* 53 (2000) 34–48.
- [9] R. Bachrach, A. Nur, A. Agnon, Liquefaction and dynamic poroelasticity in soft sediments, *J. Geophys. Res.* 106 (2001) 515–513, 526.
- [10] I.P.D. De Silva, H.J.S. Fernando, F. Eaton, D. Hebert, Evolution of Kelvin–Helmholtz billows in nature and laboratory, *Earth Planet. Sci. Lett.* 143 (1996) 217–231.
- [11] M. Gaster, E. Kit, I. Wygnanski, Large-scale structures in a forced turbulent mixing layer, *J. Fluid Mech.* 150 (1985) 23–39.
- [12] W.C. Thacker, J.W. Lavelle, Two-phase flow analysis of hindered settling, *Phys. Fluids* 20 (9) (1977) 1577–1579.
- [13] J.R. Holton, *An Introduction to Dynamic Meteorology*, Academic Press, San Diego, 1992, 511 pp.
- [14] C.M.R. Fowler, *The Solid Earth: An Introduction to Global Geophysics*, Cambridge University Press, New York, 1997, 472 pp.
- [15] A. Ayres, F. Theilen, Preliminary laboratory investigations into the attenuation of compressional and shear waves on near-surface marine sediments, *Geophys. Prospect.* 49 (1) (2001) 120–127.
- [16] O. Lioubashevski, Y. Hamiel, A. Agnon, Z. Reches, J. Fineberg, Oscillons and solitary waves in a vertically vibrated colloidal suspension, *Phys. Rev. Lett.* 83 (1999) 3190–3193.
- [17] B.F. Farrell, P.J. Ioannou, Generalized stability theory: Part I. Autonomous operators, *J. Atmos. Sci.* 53 (1996) 2025–2040.